A comparison of methods for calculating the matrix block source term in a double porosity model for contaminant transport

Clarisse Alboin, * Jérôme Jaffré, † Patrick Joly, ‡ Jean E. Roberts, §
Christophe Serres ¶

September 2, 2002

Abstract

Contaminant transport in a fractured porous medium can be modeled, under appropriate conditions, with a double porosity model. Such a model consists of a parabolic equation with a coupling term describing contaminant exchange between the fractures, which have high permeability, and the matrix block, which has low permeability. A locally conservative method based on mixed finite elements is used to solve the parabolic problem, and the calculation of the coupling term, which involves the solution of diffusion equations in the matrix blocks, is based on an analytic expression. Numerical experiments show that this semi-analytic method for the coupling term is accurate and faster than several other methods but at a small expense of computer memory.

keywords: Porous medium, fractures, double porosity

1 Introduction

The transport in a porous medium of a contaminant dissolved in a single phase fluid is governed by the transport equation

$$\begin{aligned} \omega \frac{\partial c}{\partial t} + \mathrm{div}(-D\nabla c + \mathbf{u}\, c) &= q_c \\ c(\cdot, 0) &= c^0, \end{aligned}$$

where the unknown c is the concentration of the contaminant dissolved in the fluid; the coefficients ω, D and $\mathbf{u}$ are the porosity of the medium, the diffusion coefficient, and the Darcy velocity of the fluid, respectively; the right hand side q_c is the contaminant source term; and the initial condition c^0 is the concentration of the contaminant at time $t = 0$.

*Thales, Elancourt, France, Clarisse.Alboin@thales.fr
†Inria-Rocquencourt, BP 105, 78153 Le Chesnay Cedex, France, Jerome.Jaffre@inria.fr
‡Inria-Rocquencourt, BP 105, 78153 Le Chesnay Cedex, France, Patrick.Joly@inria.fr
§Inria-Rocquencourt, BP 105, 78153 Le Chesnay Cedex, France, Jean.Roberts@inria.fr
¶IPSN, Fontenay aux Roses, France, Christophe.Serres@ipsn.fr

The Darcy velocity $\mathbf{u}$ is given by the flow equation which is Darcy's law relating the fluid pressure with the Darcy velocity $\mathbf{u}$

$$\mathbf{u} = -K\nabla p$$

together with the law of conservation of mass

$$\operatorname{div} \mathbf{u} = q.$$

Here, in Darcy's equation, the effects of gravity have been ignored. The coefficient K is the permeability of the rock; more precisely it is the permeability k divided by the viscosity μ of the fluid which might be dependent on the concentration. However here we neglect this dependence so that K is constant in time. The elliptic conservation law states that the fluid is supposed to be incompressible.

By a fracture in the porous medium is meant a very thin portion of the domain with very large permeability; very thin in comparison with the size of the domain and very permeable in comparison with the surrounding medium. Here we do not consider specific known fractures that might be included individually in the model but a network of small interconnected fractures. Also, a certain degree of regularity in the fracture network is assumed. Aside from the fact that we do not have precise information about the form or location of such a network, the difficulty for numerical modeling is a problem of scale. The scale of the fracture width and the scale of the distance between fractures in the network are very small compared to the scale of the domain size. A model that could see this kind of detail would be prohibitively large for performing calculations. However one can not neglect these fractures. There is again a difference in scale in the permeability of the fractures and the permeability of the neighboring domain so that the Darcy velocity is much larger in the fractures and they play a major role in the flow in the medium: if, for example, the source term is located in the network of fractures and vanishes after a certain time, in a first stage, the contaminant, in addition to being convected and diffused in the network of fractures, is dispersed by diffusion into the blocks of porous media, called matrix blocks, which act as reservoirs. Then in a second stage, after the concentration of contaminant in the fractures has diminished, the matrix block acts as a source as the contaminant is rediffused into the fracture system. These exchanges between matrix blocks and fractures are very significant and modify the propagation time of the contaminant [18].

These fractures must be taken into account by some sort of averaging process as in a double porosity (or dual porosity) model. The double porosity model was first described in articles [7, 22], where the model was described as a phenomenological model deduced experimentally. The model was later derived via homogenization [16, 5, 12, 17, 9]. Contaminant transport has been modeled previously using a double porosity model in [3], [4] and [13].

The model is recalled in Section 2. It consists of a transport equation in the homogenized domain coupled with a diffusion equation through a source term representing exchange between the homogenized medium and the matrix blocks.

In Section 3 standard locally conservative numerical methods based on lowest order mixed finite elements are presented. However, local conservation is required only in the homogenized medium, and is not necessary in the matrix blocks. Further, the use of standard numerical methods for the computation of the source term in the matrix blocks is very expensive. The core of this paper is then devoted to the development of a semi-analytic method for the

calculation of the source term in the matrix blocks. Similar techniques were presented in [19] and [11] but without the use of an equivalent expression for small time; see below.

In Section 4 an analytic expression of the source term describing exchange between the fractures and the matrix blocks is presented and this source term is expressed in terms of a coupling operator. This convolution form of the source term has been studied for theoretical purposes in [2]. However this expression does not lend itself naturally to numerical calculations because the convolution kernel is an infinite sum that converges very slowly for small time. A so called equivalent expression is obtained for the kernel at small time and this is used in numerical calculations for the evaluation of the kernel near the singularity at time 0.

In Section 5 the coupling operator is discretized in time. In Section 6 numerical experiments and some conclusions are given.

Throughout we have assumed that the permeability in the matrix block is sufficiently low that the transport in the matrix block is due only to diffusion.

2 The double porosity model

We consider a naturally fractured medium throughout which exists a system of interconnected fracture planes. This medium is idealized as a periodic medium as shown in Figure 1.

Homogenization for this idealized medium is carried out with a parameter ϵ equal to the ratio of the period to the size of the domain. We obtain a medium which has the average properties of the initial medium. The scale of heterogeneities is the microscopic scale and the scale of the homogenized medium is the macroscopic scale. The resulting model is composed of a concentration equation in a homogenized medium to which has been added a source term or a coupling term whose value at point x and time t is obtained by solving a diffusion equation in a matrix block associated with x. The solution acts in turn through a boundary condition as a source for the microscopic model in the matrix block. This model is the double porosity model. Two sets of parameters describe the homogenized medium: macroscopic parameters derived from the microscopic parameters in the fractures and microscopic parameters in the matrix blocks from which the coupling term is determined.

We denote by x the macroscopic variable in the homogenized medium Ω and by y the microscopic variable in a matrix block $\mathcal{Q}_x^m$ associated with the point x (Figure 2). We use the notation $\mathcal{Q}_x$ for the matrix block $\mathcal{Q}_x^m$ together with the surrounding fracture $\mathcal{Q}_x^f$ (Figure 3).

The calculation of the coupling term involves, at each point $x \in \Omega$ and for each time t, the solution of an equation modeling diffusion in a matrix block.

After homogenization, we obtain the following model: for each t and each $x \in \Omega$,

$$\begin{aligned} &\omega \frac{\partial c}{\partial t} + \operatorname{div}\left(-D\nabla c + \mathbf{u}\, c\right) = q_c - \frac{\omega_m}{|\mathcal{Q}_x|} \int_{\mathcal{Q}_x^m} \frac{\partial c^m}{\partial t}(x, y, t)\, dy \\ &c(\cdot, 0) = c^0 \end{aligned} \tag{1}$$

where the unknown c is the concentration in the homogenized medium. The scalar quantities ω, q_c and ω_m are respectively the porosity and the given source term in the homogenized medium and the porosity in the matrix block. The functions ω and q_c are related to the porosity ω^f and the source term q_c^f in the fractures by

$$\omega(x) = \frac{|\mathcal{Q}_x^f|}{|\mathcal{Q}_x|}\omega^f(x) \qquad\qquad q_c(x) = \frac{|\mathcal{Q}_x^f|}{|\mathcal{Q}_x|} q_c^f(x).$$

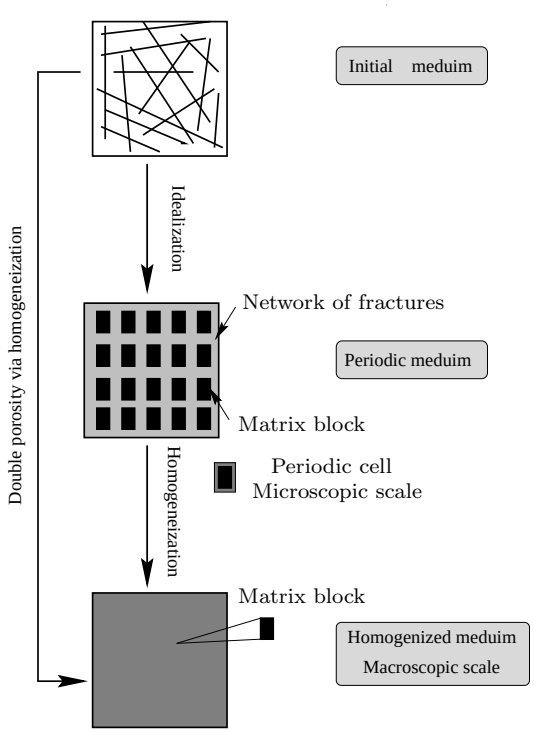

Figure 1: The double porosity model

The vector quantity D in the homogenized medium is related to that in the fractures D^f by

$$D = \frac{1}{|\mathcal{Q}_x|} \int_{|\mathcal{Q}_x^f|} (W(y) + I) dy \; D^f,$$

where $W(y)$ is the n by n matrix $W_{i,j}(y) = \dfrac{\partial w_i}{\partial y_j}$ with w_i the solution to the homogeneous Laplace equation in $\mathcal{Q}_x^f$ with a homogeneous Neuman boundary condition on $\partial\mathcal{Q}_x$ and Neuman boundary condition equal to $-n_j$, minus the j^{th} component of the normal vector on $\partial\mathcal{Q}_x^m$.

The Darcy velocity $\mathbf{u}$ in the homogenized medium is obtained from

$$\begin{aligned} \mathbf{u} &= -K\nabla p \\ \operatorname{div} \mathbf{u} &= q, \end{aligned} \tag{2}$$

where the permeability K and the source term q in the homogenized medium are given in terms of the corresponding quantities in the fractures, K^f and q^f:

$$K = \frac{1}{|\mathcal{Q}_x|} \int_{|\mathcal{Q}_x^f|} (W(y) + I) dy \; K^f, \qquad q = \frac{|\mathcal{Q}_x^f|}{|\mathcal{Q}_x|} q^f.$$

The term

$$\frac{\omega_m}{|\mathcal{Q}_x|} \int_{\mathcal{Q}_x^m} \frac{\partial c^m}{\partial t}(x, y, t)\, dy, \tag{3}$$

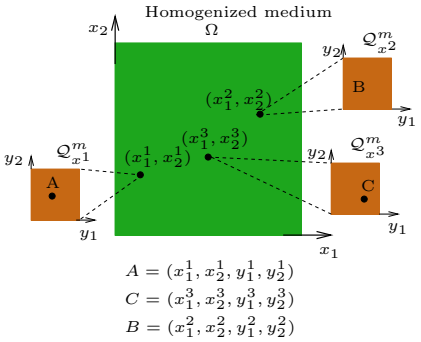

Figure 2: Systems of variables

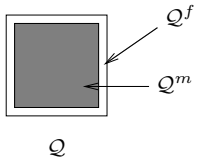

Figure 3: The fracture $\mathcal{Q}^f$ surrounding a matrix block $\mathcal{Q}^m$ and $\mathcal{Q} = \mathcal{Q}^m \cup \mathcal{Q}^f$

is the coupling term which represents the exchange between the fractures and the matrix blocks. The unknown $c^m(x, y, t)$ is the concentration at time t and at point y of the matrix block Q_x associated with x in Ω and is the solution of the contaminant transport equation on the microscopic scale. For $x \in \Omega, c^m(x, \cdot)$ is the solution of a time dependent diffusion equation in $\mathcal{Q}^m_x$:

$$\begin{aligned} &\frac{\partial c^m}{\partial t}(x, y, t) - \alpha(x)\Delta_y c^m(x, y, t) \;=\; 0, \quad y \in \mathcal{Q}^m_x, t > 0, \\ &c^m(x, y, 0) \;=\; 0, \quad y \in \mathcal{Q}^m_x, \\ &c^m(x, y, t) \;=\; c(x, t) \quad \text{on } \partial Q^m_x, \end{aligned} \tag{4}$$

where $\alpha(x)$ is the diffusion coefficient in the matrix block Q^m_x divided by the porosity ω_m in Q^m_x. Here the advection term has been neglected as the permeability is assumed to be very low in Q^m_x.

In a numerical model, equation (4) must be solved at each point x of the discretized domain Ω and at each time step which makes calculations with a double porosity model very costly with standard discretization techniques, especially as the low diffusion in the matrix block renders the problem quite stiff. This led us to calculate the coupling term analytically.

3 Numerical Approximation

We have three coupled equations to solve: the flow equation (2) and the transport equation (1) in the homogenized domain, and the diffusion equation (4) in the matrix blocks. As we have neglected the transport term in the matrix blocks, there is no need to solve for the Darcy velocity there so we do not approximate a flow equation in the matrix blocks.

We discretize the homogenized domain Ω with a structured mesh of rectangles $C \in \mathcal{T}_h$ and we denote by $E \in \mathcal{E}_h$ the edges of the mesh.

Let us consider first, the flow equation (2) in the homogenized medium Ω which is an elliptic equation. Because of our assumption that the fluid viscosity is not a function of the contaminant concentration, this equation can be solved independently and only has to be solved once. To obtain a precise approximation to the Darcy velocity and to have a locally conservative scheme we use a mixed method with the lowest order Raviart-Thomas spaces [20, 10]. The approximate pressure p_h lies in the space M_h of functions constant on each cell $C \in \mathcal{T}_h$, and the approximate velocity $\mathbf{u}_h$ lies in the space $\mathbf{W}_h$ of vector functions for which, on each cell $C \in \mathcal{T}_h$, the i^{th} component is linear in x_i and independent of x_j, if $i \neq j$, and for which, through each edge $E \in \mathcal{E}_h$, the normal component is continuous. The degrees of freedom of $\mathbf{u}_h$ are the flow rates through the edges $E \in \mathcal{E}_h$. Then the approximation equations for equation (2) are

$$\begin{aligned}
&\int_C \operatorname{div}\mathbf{u}_h \, dx = \int_{\partial C} (\mathbf{u}_h \cdot \mathbf{n}_C) dx = 0, \quad C \in \mathcal{T}_h, \\
&\int_\Omega K^{-1}\mathbf{u}_h \cdot \mathbf{v} \, dx - \int_\Omega p_h \operatorname{div}\mathbf{v} \, dx + \int_{\partial\Omega} \bar{p}\, \mathbf{v} \cdot \mathbf{n}_\Omega \, ds = 0, \quad \mathbf{v} \in \mathbf{W}_h,
\end{aligned}$$

where $\mathbf{n}_C$ and $\mathbf{n}_\Omega$ are respectively the outward normals to the boundary of C and to that of Ω. Here $\bar{p}$ is a pressure given on the boundary of Ω. If a numerical integration formula is used to evaluate the first integral of the second equation above, the resulting method is a finite volume method; cf. [21].

The transport equation (1) in the homogenized medium Ω is a diffusion-advection equation. This is the equation for which local conservation is the most important. We rewrite it as

$$\begin{aligned}
&\omega \frac{\partial c}{\partial t} + \operatorname{div}(\mathbf{w} + \mathbf{r}) = q_c - \frac{\omega_m}{|\mathcal{Q}_x|} \int_{\mathcal{Q}_x^m} \frac{\partial c^m}{\partial t}(x, y, t)\, dy \\
&\mathbf{w}_d = -D\nabla c \\
&\mathbf{w}_a = \mathbf{u}\, c
\end{aligned} \tag{5}$$

to separate the diffusion contribution from the advection contribution in order to treat these two terms differently. We treat the diffusion term again with a mixed finite element method and the advective term with a first order upstream scheme. Concerning time discretization Δt denotes the time step and we use Euler finite differences, the diffusive term being treated implicitly and the advective term being treated explicitly. On the interval $((n-1)\Delta t, n\Delta t)$ the concentration is approximated by a function $c_h^n \in M_h$ and the vector function $\mathbf{w}_d$ by $\mathbf{w}_{dh}^n \in \mathbf{W}_h$. Then equation (5) is approximated by

$$\begin{aligned}
&\int_C \omega \frac{c_h^{n+1} - c_h^n}{\Delta t}\, dx + \int_{\partial C} \left(\mathbf{w}_{dh}^{n+1}\, dx + (c_h^-)^n \mathbf{u}_h\right) \cdot \mathbf{n}_C \, dx \\
&\qquad = \left(\int_C \left(q_c - \frac{\omega_m}{|\mathcal{Q}_x|} \int_{\mathcal{Q}_x^m} \frac{\partial c^m}{\partial t}(x, y, t)\, dy \right) dx \right)^{n+1}, \quad C \in \mathcal{T}_h, \\
&\int_\Omega D^{-1}\mathbf{w}_{dh} \cdot \mathbf{v}_h \, dx - \int_\Omega c_h^{n+1} \operatorname{div}\mathbf{v}_h \, dx + \int_{\partial\Omega} \bar{c}^{n+1}\, \mathbf{v}_h \cdot \mathbf{n}_\Omega \, ds = 0, \\
&\qquad\qquad \mathbf{v}_h \in \mathbf{W}_h,
\end{aligned}$$

where c_h^- denotes the upstream concentration with respect to the velocity $\mathbf{u}_h$ and c_d^{n+1} a given concentration on the boundary of Ω. Here the superscript in the right hand side of

the first equation indicates an approximation to this term at time $n+1$. Again the use of a numerical integration formula for the first integral in the second equation results in a finite volume method.

Finally the source term (3) must be calculated at each time step and at each point of discretization. Standard discretization techniques could be used to approximate the solution of the matrix block equations (4). However, in addition to the fact that equation (4) must be solved $N_t \times M$ times, where N_t is the number of time steps and M the number of discretisation points, the fact that the coefficient α is in general quite small renders the problem stiff. But, since we do not need to use a locally conservative scheme in the matrix blocks and because in each block the coefficient as well as the data is constant in space and the geometry of the block $\mathcal{Q}_x^m$, a rectangle, is simple, we can use a semi-analytical method for calculating an approximate solution of equation (4). We describe this method below.

4 Analytic expression of the coupling term

We now give an analytic expression of the coupling term in terms of a convolution kernel written as a series. For simplicity's sake, we have taken $\mathcal{Q}_x^m$ to be a square instead of a general rectangle.

With $\hat{c}^m(x,y,t) = c^m(x,y,t) - c(x,t)$, $\hat{c}^m$ is the solution of

$$\begin{aligned}
&\frac{\partial \hat{c}^m}{\partial t}(x,y,t) - \alpha(x)\Delta_y \hat{c}^m(x,y,t) \;=\; \frac{\partial c}{\partial t}(x,t), \quad y \in \mathcal{Q}_x^m,\ t>0,\\
&\hat{c}^m(x,y,0) \;=\; -c(x,0) \ \text{ in } \mathcal{Q}_x^m\\
&\hat{c}^m(x,y,t) \;=\; 0 \quad \text{ on } \partial\mathcal{Q}_x^m.
\end{aligned}$$

If $\mathcal{Q}_x^m$ is identified with $[-\frac{k}{2},\frac{k}{2}]^2$, the function $\hat{c}^m$ may be expressed in terms of the spectral basis $\{\omega_{p,q} \,:\, p,q \,=\, 1,2,\cdots\}$, where $\omega_{p,q}(y) = \omega_p(y_1)\omega_q(y_2)$ and ω_p is the solution on $[-\frac{k}{2},\frac{k}{2}]$ of

$$-\omega_p'' = \frac{\pi^2 p^2}{k^2}\omega_p, \qquad \omega_p(-\frac{k}{2}) = \omega_p(\frac{k}{2}) = 0,$$

with coefficients $\hat{c}_{p,q}^m$ solutions of the ordinary differential equation

$$\frac{\partial \hat{c}_{p,q}^m}{\partial t}(x,t) + \alpha_{p,q}\hat{c}_{p,q}^m(x,t) = -\frac{\partial c}{\partial t}(x,t)\mu_{p,q},$$

with

$$\alpha_{p,q} = \frac{\alpha\pi^2}{k^2}(p^2+q^2) \qquad \text{and} \qquad \mu_{p,q} = \int_{\mathcal{Q}_x^m} \omega_{p,q}. \tag{6}$$

Thus we have

$$\hat{c}^m(x,y,t) = \sum_{p,q\geq 1} \hat{c}_{p,q}^m(x,t)\omega_{p,q}(y), \tag{7}$$

with

$$\omega_p(y_i) = \begin{cases} \sqrt{\frac{2}{k}}\sin(\frac{p\pi y_i}{k}) & \text{if } p \text{ is even} \\ \sqrt{\frac{2}{k}}\cos(\frac{p\pi y_i}{k}) & \text{if } p \text{ is odd,} \end{cases} \qquad i=1,2,$$

and

$$\hat{c}^m_{p,q}(x,t) = -\mu_{p,q}\left(\int_0^t \frac{\partial c}{\partial t}(x,s)e^{-\alpha_{p,q}(t-s)}ds + c(x,0)e^{-\alpha_{p,q}t}\right).$$

A simple calculation then shows that the coupling term is given by

$$\int_{\mathcal{Q}^m_x} \frac{\partial c^m}{\partial t}(x,y,t)\,dy \\ = \sum_{p,q} \mu^2_{p,q}\alpha_{p,q}\left(\int_0^t \frac{\partial c}{\partial t}(x,s)e^{-\alpha_{p,q}(t-s)}ds + c(x,0)e^{-\alpha_{p,q}t}\right),$$

or, defining the convolution kernel $K_\alpha(t)$,

$$K_\alpha(t) = \sum_{p,q} \mu^2_{p,q}\alpha_{p,q}e^{-\alpha_{p,q}t}, \quad \text{if } t > 0 \ , \tag{8}$$

by

$$\int_{\mathcal{Q}^m_x} \frac{\partial c^m}{\partial t}(x,y,t)\,dy = \int_0^t \frac{\partial c}{\partial t}(x,s)K_\alpha(t-s)ds + c(x,0)K_\alpha(t). \tag{9}$$

As in [2] one can express the coupling term (9) in terms of a coupling operator S_α. For α a function from Ω to $\mathbb{R}^+$, let $\mathcal{S}_\alpha$ be the operator

$$\begin{array}{rccl} \mathcal{S}_\alpha \ : & H^1(0,T;L^2(\Omega)) & \longrightarrow & L^2(0,T;L^2(\Omega)) \\ & c & \longrightarrow & \mathcal{S}_\alpha(c), \end{array} \tag{10}$$

where

$$\mathcal{S}_\alpha(c)(x,t) = \omega_m \int_0^t \frac{\partial c}{\partial t}(x,s)K_\alpha(t-s)ds + \omega_m c(x,0)K_\alpha(t).$$

With this notation, problem (1) can be rewritten as follows:

$$\begin{array}{l} \dfrac{\partial c}{\partial t} + \mathrm{div}_x[-D(x)\nabla_x c + u(x)c] + \mathcal{S}_\alpha(c) \ = \ q_c \\ c(x,0) \ = \ c^0(x). \end{array} \tag{11}$$

Even though we have an analytic expression for $S_\alpha(c)$ we do not have a closed form expression. Thus in addition to deciding whether this term should be treated implicitly or explicitly we must approximate the time integral in the convolution term, approximate the time derivative in this term, and approximate the convolution kernel which is given as an infinite sum. We first investigate some of the properties of the kernel K_α and of the operator S_α.

Lemma 1 *The series K_α converges on $(0,+\infty)$ and converges uniformly on the subinterval $[\varepsilon,+\infty)$ for each $\varepsilon > 0$. Moreover, for $\alpha \in \mathbb{R}^+$ given, K_α has the following behavior as t decreases toward 0:*

$$K_\alpha(t) = 4\sqrt{\frac{|\mathcal{Q}^m|\alpha}{\pi t}} - \frac{16\alpha}{\pi} + O(t). \tag{12}$$

PROOF:
First, calculating that

$$\mu_{p,q} = \begin{cases} \pm\dfrac{8\,k}{pq\pi^2} & \text{if } p \text{ and } q \text{ are odd} \\ 0 & \text{otherwise} \end{cases},$$

we see that $\mu_{p,q}^2\alpha_{p,q} \leq \dfrac{128\alpha}{\pi^2}$. Thus, for each $\varepsilon > 0$, there is a positive constant C_ε such that

$$K_\alpha(t) \leq \frac{128\alpha}{\pi^2} \sum_{p,q\geq 1} e^{-\alpha_{p,q}t} \leq C_\varepsilon e^{-\frac{\alpha\pi^2}{k^2}t}, \quad \forall t \geq \varepsilon,$$

and we see that $K_\alpha(t)$ is a series that converges on $(0,\infty)$ and converges uniformly on $[\varepsilon,\infty)$ for each positive ε.

Then a straightforward calculation shows that

$$K_\alpha(t) = -2\zeta(t)\zeta'(t) \tag{13}$$

with $\zeta(t) = \sum_{p\geq 1} \mu_p^2 e^{-\frac{\alpha\pi^2}{k^2}p^2 t}$.

One can now rewrite $\zeta(t)$ as follows:

$$\zeta(t) \;=\; \int_{-\frac{k}{2}}^{\frac{k}{2}} z(y,t)\,dy,$$

where $z(y,t)$ is the solution of

$$\begin{aligned} &\frac{\partial z}{\partial t} - \alpha\frac{\partial^2 z}{\partial y^2} \;=\; 0, \quad -k/2 \leq y \leq k/2, \\ &z(y,0) \;=\; -1, \qquad -k/2 \leq y \leq k/2, \\ &z(\pm k/2, t) \;=\; 0. \end{aligned}$$

Then $z(y,t)$ can be identified with the restriction to the segment $[-k/2, k/2]$ of the solution $\tilde{z}(y,t)$ of

$$\begin{aligned} &\frac{\partial \tilde{z}}{\partial t} - \alpha\frac{\partial^2 \tilde{z}}{\partial y^2} = 0, \quad y \in \mathbb{R},\, t > 0, \\ &\tilde{z}(y,0) = \sum_{l=-\infty}^{l=\infty} (-1)^{l+1}\,\chi(y - lk), \quad y \in \mathbb{R}, \end{aligned}$$

where χ is the characteristic function of the interval $[-k/2, k/2]$. One may also write $\tilde{z}(y,t)$ as an infinite sum:

$$\tilde{z}(y,t) \;=\; \sum_{l=-\infty}^{l=\infty} (-1)^{l+1} z_l(y,t)$$

with $z_l(y,t)$ the solution of

$$\begin{aligned} &\frac{\partial z_l}{\partial t} - \alpha\frac{\partial^2 z_l}{\partial y^2} = 0, \quad y \in \mathbb{R},\, t > 0, \\ &z_l(y,0) = \chi(y - lk), \quad y \in \mathbb{R}; \end{aligned}$$

that is

$$z_l(y,t) \;= \frac{1}{2\sqrt{\pi\alpha t}} \int_{kl-k/2}^{kl+k/2} e^{-\frac{(y-\eta)^2}{4t\alpha}} d\eta.$$

Introducing

$$\zeta_l(t) = \int_{-k/2}^{k/2} z_l(y,t) dy,$$

one has

$$\zeta(t) = \sum_{l=-\infty}^{l=\infty} (-1)^{l+1}\, \zeta_l(t).$$

If $\eta \in [lk - k/2, lk + k/2]$ and $y \in [-k/2, k/2]$, then $k(l-1) \leq \eta - y \leq k(l+1)$, so that

$$|\zeta_l(t)| \leq \frac{k^2}{2\sqrt{\pi\alpha t}}\, e^{-\frac{k^2(l-1)^2}{4t\alpha}}. \tag{14}$$

Thus

$$\begin{aligned} \sum_{l\geq 2} |\zeta_l(t)| &\leq \frac{k^2}{2\sqrt{\pi\alpha t}} \sum_{l\geq 2} e^{-\frac{k^2(l-1)^2}{4t\alpha}} \leq \frac{k^2}{2\sqrt{\pi\alpha t}} \sum_{l\geq 1} e^{-\frac{k^2 l^2}{4t\alpha}} \\ &\leq \frac{k^2}{2\sqrt{\pi\alpha t}}\, e^{-\frac{k^2}{4t\alpha}} \sum_{l\geq 1} e^{-\frac{k^2(l^2-1)}{4t\alpha}}. \end{aligned}$$

Since for $l \geq 1$ we have $l^2 - 1 \geq 2(l-1)$ and we obtain

$$\sum_{l\geq 2} |\zeta_l(t)| \leq \frac{k^2}{2\sqrt{\pi\alpha t}}\, e^{-\frac{k^2}{4t\alpha}} \sum_{l\geq 0} e^{-\frac{2k^2 l}{4t\alpha}} \leq \frac{k^2}{2\sqrt{\pi\alpha t}}\, \frac{e^{-\frac{k^2}{4t\alpha}}}{1 - e^{-\frac{k^2}{2t\alpha}}}. \tag{15}$$

One clearly has the same upper bound for $\sum_{l\leq -2} |\zeta_l(t)|$. From inequalities (14),(15) one obtains that the series $\sum_{|l|\geq 2} \zeta_l(t)$ is uniformly convergent on $[0,\infty)$ and vanish when $t \to 0$. Similar calculations show that the series of the derivatives at any order are also uniformly convergent on $[0,\infty)$ and vanish when $t \to 0$. Therefore we can conclude that the series $\sum_{|l|\geq 2} \zeta_l(t)$ is $\mathcal{C}^\infty$ on $[0,\infty)$ with all of its derivatives vanishing at 0.

We next consider ζ_1 and ζ_{-1}. The function ζ_1 is given by

$$\zeta_1(t) = \frac{1}{2\sqrt{\pi\alpha t}} \int_{-k/2}^{k/2} \int_{k/2}^{3k/2} e^{-\frac{(y-\eta)^2}{4t\alpha}} d\eta\, dy$$

or, denoting by u and v respectively, $\eta - y$ and $\eta + y$,

$$\begin{aligned} \zeta_1(t) &= \frac{1}{4\sqrt{\pi\alpha t}} \left[\int_0^k \int_{k-u}^{k+u} e^{-\frac{u^2}{4t\alpha}} dv\, du + \int_k^{2k} \int_{-k+u}^{3k-u} e^{-\frac{u^2}{4t\alpha}} dv\, du \right] \\ &= \frac{1}{2\sqrt{\pi\alpha t}} \left[\int_0^k e^{-\frac{u^2}{4t\alpha}} u du - \int_k^{2k} e^{-\frac{u^2}{4t\alpha}} (u - 2k)\, du \right]. \end{aligned}$$

Now letting $u = \sqrt{t\alpha}\, s$ one obtains

$$\zeta_1(t) = \frac{1}{2\sqrt{\pi\alpha t}} \left[t\alpha \int_0^{\frac{k}{\sqrt{t\alpha}}} e^{-\frac{s^2}{4}}\, s\, ds - \sqrt{t\alpha} \int_{\frac{k}{\sqrt{t\alpha}}}^{\frac{2k}{\sqrt{t\alpha}}} e^{-\frac{s^2}{4}} (\sqrt{t\alpha} s - 2k)\, ds \right].$$

Thus, as

$$\int_0^{\frac{k}{\sqrt{t\alpha}}} e^{-\frac{s^2}{4}}\, s\, ds = -2(e^{-\frac{k^2}{4t\alpha}} - 1)$$

and

$$\begin{aligned} \left| \int_{\frac{k}{\sqrt{t\alpha}}}^{\frac{2k}{\sqrt{t\alpha}}} e^{-\frac{s^2}{4}} (\sqrt{t\alpha} s - 2k) ds \right| &\leq e^{-\frac{k^2}{4t\alpha}} \left| \int_{\frac{k}{\sqrt{t\alpha}}}^{\frac{2k}{\sqrt{t\alpha}}} (\sqrt{t\alpha} s - 2k) ds \right| \\ &\leq e^{-\frac{k^2}{4t\alpha}} \frac{3k^2}{2\sqrt{t\alpha}}, \end{aligned}$$

one can conclude that $\zeta_1(t) - \sqrt{\dfrac{t\alpha}{\pi}}$ is $\mathcal{C}^\infty$ on $[0, \infty)$ with all of its derivatives vanishing at 0. Similarly one may show that $\zeta_{-1}(t) - \sqrt{\dfrac{t\alpha}{\pi}}$ is $\mathcal{C}^\infty$ on $[0, \infty)$ with all of its derivatives vanishing at 0.

There remains to calculate ζ_0:

$$\zeta_0(t) = \frac{1}{2\sqrt{\pi\alpha t}} \int_{-k/2}^{k/2} \int_{-k/2}^{k/2} e^{-\frac{(y-\eta)^2}{4t\alpha}} d\eta\, dy.$$

With u and v as before one has

$$\begin{aligned} \zeta_0(t) &= \frac{1}{\sqrt{\pi\alpha t}} \left[\int_0^k \int_0^{k-u} e^{-\frac{u^2}{4t\alpha}} dv\, du + \int_k^{2k} \int_{u-k}^{3k-u} e^{-\frac{u^2}{4t\alpha}} dv\, du \right] \\ &= \frac{1}{\sqrt{\pi\alpha t}} \left[\int_0^k k e^{-\frac{u^2}{4t\alpha}} du - \int_0^k e^{-\frac{u^2}{4t\alpha}} u\, du \right]. \end{aligned}$$

We note that

$$\int_0^k e^{-\frac{u^2}{4t\alpha}} u\, du = 2\alpha t \left(1 - e^{-\frac{1}{4t\alpha}}\right).$$

As before letting $u = \sqrt{t\alpha}\, s$ one obtains

$$\int_0^k k e^{-\frac{u^2}{4t\alpha}} du = k\sqrt{t\alpha} \left(\int_0^\infty e^{-\frac{s^2}{4}} ds - \int_{\frac{k}{\sqrt{t\alpha}}}^\infty e^{-\frac{s^2}{4}} ds \right).$$

Now, as

$$\int_0^\infty e^{-\frac{s^2}{4}} ds = \sqrt{\pi}$$

and

$$\int_{\frac{k}{\sqrt{t\alpha}}}^\infty e^{-\frac{s^2}{4}} ds \geq \int_{\frac{k}{\sqrt{t\alpha}}}^{\frac{2k}{\sqrt{t\alpha}}} \geq e^{-\frac{k^2}{t\alpha}} \frac{k}{\sqrt{t\alpha}},$$

one obtains

$$\int_0^k k e^{-\frac{u^2}{4t\alpha}} du \leq k\sqrt{t\alpha} \left(\sqrt{\pi} - e^{-\frac{k^2}{t\alpha}} \frac{k}{\sqrt{t\alpha}} \right).$$

and $\zeta_0(t) - k + 2\sqrt{\frac{t\alpha}{\pi}}$ is $\mathcal{C}^\infty$ on $[0,\infty)$ vanishing along with all of its derivatives at 0.

Thus one may conclude that $\zeta(t) + k - 4\sqrt{\dfrac{t\alpha}{\pi}}$ is $\mathcal{C}^\infty$ on $[0,\infty)$ vanishing along with all of its derivatives at 0. Then using expression (13) of $K_\alpha(t)$ we finally obtain equality (12).

The following lemma describes the behavior of $K_\alpha(t)$ for large t.

Lemma 2 *As t increases away from 0, the kernel K_α decreases rapidly,*

$$K_\alpha(t) \leq C\, e^{\frac{-2\alpha\pi^2 t}{|\mathcal{Q}^m|}}. \tag{16}$$

This lemma is an immediate consequence of the definition of the kernel (8),(6).

In practice, expression (12) for K_α is very useful for evaluating K_α in a neighborhood of the singularity at 0 since the series in (8) converges very slowly for small t. Estimate (16) indicates that, for large t, calculating only a few terms of this series is sufficient.

Remark 1 *As in [1], one can show that the operator $\mathcal{S}_\alpha$ is pseudo-differential in time of order $1/2$, in the sense that, for all $s < \frac{1}{2}$,*

$$\mathcal{S}_\alpha \ : \ H^s(\mathbb{R}^+; L^2(\Omega)) \longrightarrow H^{s-\frac{1}{2}}(\mathbb{R}^+; L^2(\Omega));$$

cf. also theorem 2 of [2].

Remark 2 *The operator, $\mathcal{S}_\alpha$, is also semi-positive in the sense that for almost every $x \in \Omega$*

$$\int_0^T \mathcal{S}_\alpha(c)(x,s)c(x,s)ds \geq 0; \tag{17}$$

this is shown in [2, 19]. Another useful property is that

$$\int_0^T \mathcal{S}_\alpha(c)(x,s)\frac{\partial c(x,s)}{\partial s}ds \geq 0. \tag{18}$$

These two inequalities are useful to establish bounds on the solution that lead to show existence, uniqueness and regularity results through the use of standard analysis techniques.

5 Numerical approximation of the coupling operator

5.1 Time discretization

Let $\Delta t = \dfrac{T}{N_t}$, T the final time of the experiment, be the length of the time step in the homogenized medium. The semi-discretization in time of equation (11) is given by

$$\frac{c^{n+1} - c^n}{\Delta t} + \operatorname{div}(-D\nabla c^{n+1} + \mathbf{u}\, c^n) + (S_\alpha c)^{n+\frac{1}{2}} \ = \ q_c^{n+1}, \tag{19}$$

where the approximation $(S_\alpha c)^{n+\frac{1}{2}}$ of the coupling term, at a point $x \in \Omega$, is given by

$$(S_\alpha c)^{n+\frac{1}{2}}(x) = [\sum_{j=0}^{n} K_{nj}(c^{j+1}(x) - c^j(x)) + \ K_n c^0(x)]\ \frac{1}{|\mathcal{Q}_x|}, \tag{20}$$

and where for all $n,\ n = 0, ..., N_t - 1$,

$$\begin{aligned} K_{nj} &= \int_{n\Delta t}^{(n+1)\Delta t} \int_{j\Delta t}^{(j+1)\Delta t} \frac{K_\alpha(t-s)}{(\Delta t)^2}\, ds\, dt, \quad \forall j = 0, ..., n-1, \\ K_{nn} &= \int_{n\Delta t}^{(n+1)\Delta t} \int_{n\Delta t}^{t} \frac{K_\alpha(t-s)}{(\Delta t)^2}\, ds\, dt\ , \\ K_n &= \int_{n\Delta t}^{(n+1)\Delta t} \frac{K_\alpha(t)}{\Delta t}\, dt. \end{aligned} \tag{21}$$

This discretization in time is chosen in order to guarantee the stability of the scheme. In fact, the discretization in time of the coupling term satisfies the stability condition

$$\sum_{n=0}^{N_t-1} (\mathcal{S}_\alpha c)^{n+\frac{1}{2}}\, \frac{c^{n+1}(x) - c^n(x)}{\Delta t} \Delta t \geq 0. \tag{22}$$

This inequality may be checked by setting

$$c_{\Delta t}(x,t) \ = \ \sum_{l=0}^{N_t} c^l(x) \beta_l(t), \tag{23}$$

where β_l is a hat function; i.e. the piecewise linear function on $[0, T]$ determined by $\beta_l(j\Delta t) = \delta_{j,l},\ j = 0, \ldots, N_t$. and noting that

$$\frac{\partial\, c_{\Delta t}}{\partial t}(x,t) \ = \ \sum_{l=0}^{N_t-1} \frac{c^{l+1}(x) - c^l(x)}{\Delta t} \zeta_{l+1/2}(t), \tag{24}$$

where $\zeta_{l+1/2}(t)$ is the characteristic function

$$\zeta_{l+1/2}(t) \ = \ \begin{cases} 1 & \text{on } [l\,\Delta t, (l+1)\Delta t] \\ 0 & \text{otherwise.} \end{cases}$$

From (18), we have

$$\int_0^T \mathcal{S}_\alpha(c_{\Delta t})(x,t) \frac{\partial c_{\Delta t}(x,t)}{\partial t}\, dt \geq 0.$$

If we substitute for $c_{\Delta t}$ and $\dfrac{\partial c_{\Delta t}}{\partial t}$ their expressions given in (23) and (24), we obtain inequality (22).

5.2 Implementation considerations

To calculate the integrals in equations (21) we first note that using a change of variables one may write

$$\begin{aligned} K_{nj} &= \int_{(n-(j+1))\Delta t}^{(n-j)\Delta t} \frac{K_\alpha(r)}{(\Delta t)^2}(r-(n-(j+1))\Delta t)\,dr+ \\ &\quad \int_{(n-j)\Delta t}^{((n+1)-j)\Delta t} \frac{K_\alpha(r)}{(\Delta t)^2}(-r+((n+1)-j))\Delta t)\,dr,\ 0\le j<n, \\ K_{nn} &= \int_0^{\Delta t} \frac{K_\alpha(r)}{(\Delta t)^2}(\Delta t-r)\,dr, \end{aligned}$$

and that K_{nj} can actually be indexed by a single index $m = n - j > 0$.

Close to 0, the convolution kernel K_α is actually replaced by its equivalent form given in (12) for which the integrals can be computed exactly.

Away from 0, the integrals can be calculated by truncating the series (8) and calculating exactly the integrals corresponding to the remaining terms of the sum. These terms are actually very few since they vanish very quickly when p and q increase.

Truncating the series (8) means also that we have set $K_\alpha = 0$ for t large which implies $K_{nj} = 0$ for j not close to n. Therefore we replace the sum $\sum_{j=0}^{n}$ by $\sum_{j=n-M}^{n}$ in (20):

$$(S_\alpha c)_M^{n+\frac{1}{2}}(x) = \left[\sum_{j=n-M}^{n} K_{nj}(c^{j+1}(x)-c^j(x)) + K_n c^0(x)\right] \frac{1}{|\mathcal{Q}_x|}, \tag{25}$$

and M becomes a parameter of approximation.

The choice of the time interval on which K_α is actually replaced by its equivalent form and the choice of the number of terms left in the truncated series, which corresponds to a choice of M, are adjusted by trial and error to the problem under consideration. Automatic determination of these parameters would require more numerical analysis. Some considerations on the choice of M can be found in [19].

We also point out that calculating with (25) requires the storage in memory of the concentration at only M time steps.

We conjecture that the discretized coupling term expressed with the truncated kernel satisfies as well the stability condition

$$\sum_{n=0}^{N_t-1} (\mathcal{S}_\alpha c)_M^{n+\frac{1}{2}} \frac{c^{n+1}(x)-c^n(x)}{\Delta t}\Delta t \ge 0.$$

6 Numerical experiments

We present two numerical experiments. The first numerical experiment validates the numerical model by comparison with the Grisak laboratory experiment. In the second numerical experiment we compare the semi-analytic method presented above with standard space-time discretization methods for the calculation in the matrix blocks.

6.1 The Grisak experiment

This experiment consists in injecting a chloride tracer into a cylinder of quasi-regular fractured porous rock [15]. The fractures are distributed along two orthogonal directions, one parallel to the axis of revolution of the cylinder. The cylinder is saturated with water and the velocity of the fluid is maintained constant and parallel to the axis of revolution of the cylinder. The tracers are injected into the network of fractures at one end of the cylinder, the relative concentration depending on time is measured at the other end of the cylinder. The microscopic parameters, characterizing the rock and the network of fractures are given in Table 1. The

Parameters	*Matrix block*	*Fracture network*
Darcy velocity ($cm\,s^{-1}$)	0	$3.4375\,10^{-2}$
Longitudinal dispersion (cm)	-	4
Transversal dispersion (cm)	-	0
Molecular diffusion ($cm^2\,s^{-1}$)	$5\,10^{-7}$	$5\,10^{-7}$
Porosity	0.35	-
Fracture aperture (cm)	-	$8\,10^{-3}$
Space between fractures (cm)	-	4

Table 1: Parameter values for Grisak's experiment

period of simulation is 4 days discretized with 4500 time steps. Figure 4 shows the calculated relative concentration at the outflow end of the cylinder and compares it with an analytical solution given in [15] and with experimental measurements. One can observe that there is good agreement of the three curves, especially that calculated with the double porosity model and that calculated from an analytic expression. Discrepancies between these two curves and the experimental one are due to the mathematical model itself.

To illustrate the importance of the coupling term, we simulate the transport of tracers in two cases, when neglecting the coupling term, that is without matrix diffusion, and when taking it into account, that is with matrix diffusion. The results are shown in Figure 5, where the calculated concentrations are shown at a given time, and in Figure 6, where the concentrations at a given point are shown as functions of time. These figures show that for the given data the effect of matrix diffusion is significant. The double porosity model actually smears the contaminant front which would be too sharp if a single porosity model were used.

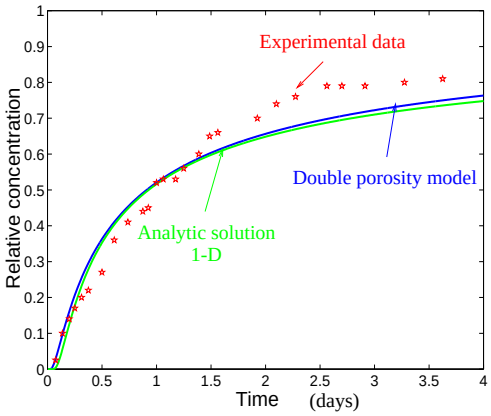

Figure 4: Relative concentrations at the outflow end of the cylinder as functions of time in the Grisak experiment

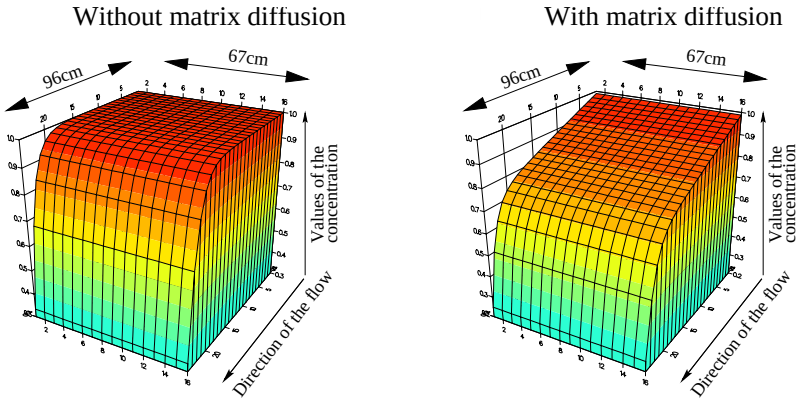

Figure 5: Concentration at 4 days, on a cross-section of the homogenized medium for data given in Table 1

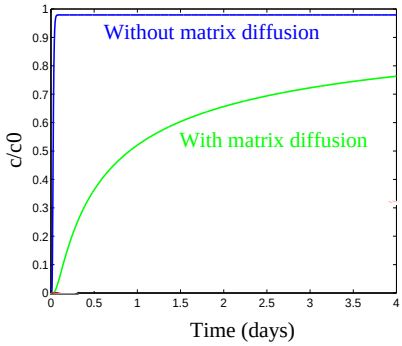

Figure 6: Relative concentration at a point of the homogenized medium for data given in Table 1

6.2 A comparison of different methods for calculating the coupling term

To compare different methods for calculating the coupling term, we consider a simple experiment where a contaminant is transported in a square domain only by diffusion. Initially, we have a positive concentration at the center of the domain. The data for this experiment are given in Table 2. They correspond to a stiff problem, the ratio of the diffusion coefficient in the fracture network to that in the matrix blocks being equal to 100.

Parameters	*Matrix block*	*Fracture network*
Molecular diffusion ($cm^2\, s^{-1}$)	10^{-6}	10^{-4}
Porosity	1	1
Fracture aperture (cm)	-	0.1
Space between fractures (cm)	-	10

Table 2: Parameter values for experiments comparing methods of calculating the coupling term

The period of simulation is $4.5\,10^7$ seconds discretized with 900 time steps. We compare the run time and the memory space using four methods to calculate the coupling term: mixed finite elements with the lowest order Raviart-Thomas spaces [20, 10], cell-centered finite volumes [14] also called the integral form of the finite difference method [6], both with a uniform grid, a spectral method (cf. [8]) and the semi-analytic method described above. The first two methods are locally conservative while the latter two are only globally conservative. However local conservation is important only for the transport equation in the homogenized medium but not for the calculations in the matrix block which need be only globally conservative, so the last two methods are also appropriate for the matrix blocks.

One difficulty in this experiment is that in the matrix blocks located where the contaminant front propagates we have to solve a parabolic problem with a large jump between the boundary concentration values and the concentration values inside the matrix block, giving rise to stiff boundary layers (see a sketch in Figure 7). For such problems, the mixed finite element method is not appropriate since it does not satisfy the maximum principle and gives oscillations in the neighborhood of the boundary layer, unless a large number of discretization

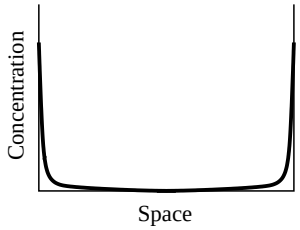

Figure 7: A stiff boundary layer problem arising in some matrix block calculations

points is put in the boundary layer. With the coarse discretizations that we used it was not possible to get a reasonable answer, and this method was dropped from the comparison.

In Figure 8 we show a comparison between the semi-analytic method, the cell-centered finite volume method with a uniform grid and the spectral method. This comparison shows that the finite volume method is slow to converge which makes it very expensive. On the contrary the spectral method converges quickly since it naturally puts more degrees of freedom close to the boundary. One could of course improve the performance of the finite volume method by using a nonuniform grid. This we have not done however, as in this setting, homogeneous data with a simple geometry and constant boundary data, the spectral method should outperform the finite volume method even when a nonuniform grid is used for the latter.

Figure 8: Values of the coupling term as functions of time at some point of the domain Ω for various methods of calculating the coupling term

Table 3 gives a comparison in terms of costs, computing time (measured in hours, minutes and seconds) and memory (measured in Megabytes). The last column gives a quantitative expression of what is shown in Figure 8. It gives the relative L^2 error over time in the coupling term at a given point, where the semi-analytic solution is used as the reference. As we can see, the semi-analytical method presented above is much cheaper in terms of computing time. It is somewhat more expensive in terms of memory space since for this stiff problem it is necessary to store the concentration at a large number of time steps (1/3 of 900 time steps).

Method	*Run time*	*Memory space*	*Coupling term error*
Finite volumes (10*10)	11'07"	16 Mb	0.28
Finite volumes (20*20)	1h47'	19 Mb	0.1
Finite volumes (30*30)	8h26'	25 Mb	$5\ 10^{-2}$
Spectral method (9*9)	6'31"	16 Mb	$3.46\ 10^{-2}$
Semi-analytical method	2'23"	28 Mb	-

Table 3: Comparison of different methods for calculating the coupling term (stiff case)

We also looked at a smoother case where the diffusion coefficient in the matrix blocks is now only 10^{-5} (instead of 10^{-6} before) so the ratio of the diffusion coefficients in the fracture

network to that in the matrix blocks is now equal to 10 (instead of 100). Results are shown in table 4. The calculation with the semi-analytic method is now cheaper in terms of memory cost than in the stiff case since the number of terms in the sum (25) required to calculate the coupling term is smaller (70 out of 900). One should note that in this case a much coarser grid can be used for the finite volume method.

Method	*Run time*	*Memory space*	*Coupling term error*
Finite volumes (10*10)	12'49"	16 Mb	$2.8\ 10^{-2}$
Spectral method (9*9)	8'16"	16 Mb	$1.6\ 10^{-2}$
Semi-analytical method	1'04"	19 Mb	-

Table 4: Comparison of different methods for calculating the coupling term (smooth case)

We mention that no extraordinary measures have been taken for the optimization of the performance of any of the codes used in these tests so the results can only be taken as indicative.

7 Conclusion

In a fractured porous medium with numerous interconnected fractures, the contaminant transfer between matrix blocks and fractures may be very significant. This transfer is taken into account in a double porosity model with a term coupling the homogenized medium with matrix blocks. We have shown how to calculate this term with the semi-analytical method. Numerical experiments have shown the efficiency of this new numerical procedure in comparison with standard discretizations which could be used in the matrix blocks .

References

[1] C. Alboin, J. Jaffré, P. Joly, and J. Roberts, *On a convolution operator arising in a double porosity model*, Tech. Rep. 4126, INRIA, BP 105, 78153 Le Chesnay cedex, France, 2001.

[2] T. Arbogast, *Analysis of the simulation of single phase flow through a naturally fractured reservoir*, SIAM J. Numer. Anal., 26 (1989), pp. 12–29.

[3] ——, *On the simulation of incompressible, miscible displacement in a naturally fractured reservoir*, R.A.I.R.O. Model. Mathem. Anal. Numer., 23 (1989), pp. 5–51.

[4] ——, *Gravitational forces in dual-porosity systems : 1. model derivation by homogenization*, Transport in Porous Media, 13 (1993), pp. 179–203.

[5] T. Arbogast, J. Douglas, Jr., and U. Hornung, *Derivation of the double porosity model of single phase flow via homogenization theory*, Siam J. Math. Anal., 21 (1990), pp. 823–836.

[6] K. Aziz and A. Settari, *Petroleum reservoir simulation*, Applied Science Publishers, London, 1991.

[7] G. Barenblatt, I. Zheltov, and I. Kochina, *Basic concepts in the theory of seepage of homogeneous liquids in the fractured rock*, J. Appl. Math. Mech., 24 (1960), pp. 1286–1303.

[8] C. Bernardi and Y. Maday, *Approximations spectrales de problèmes aux limites elliptiques*, vol. 10 of Mathematiques & Applications, Springer-Verlag France, Paris, 1992.

[9] A. Bourgeat, S. Luckhaus, and A. Mikelic, *Convergence of the homogenization process for a double-porosity model of immiscible two-phase flow.*, SIAM J. Math. Anal., 27 (1996), pp. 1520–1543.

[10] F. Brezzi and M. Fortin, *Mixed and Hybrid Finite Element Methods*, Springer-Verlag, Berlin, 1991.

[11] A. de Swaan, *Theory of waterflooding in fractured reservoirs*, Soc. Petroleum Engr. J., 18 (1978), pp. 117–122.

[12] J. Douglas, Jr. and T. Arbogast, *Dual porosity models for flow in naturally fractured reservoirs*, in Dynamics of fluids in hierarchical porous formations, J. Cushman, ed., Academic press, London, 1990, pp. 177–221.

[13] J. Douglas, Jr. and A. M. Spagnuolo, *The transport of nuclear contamination in fractured porous media*, Journal of Korean Math. Soc., 38 (2001), pp. 723–761.

[14] R. Eymard, T. Gallouët, and R. Herbin, *Finite volume methods*, in Handbook of Numerical Analysis Vol. VII, P. Ciarlet and J. Lions, eds., North Holland, Amsterdam, 2000, pp. 713–1020.

[15] G. Grisak, J. Pickens, and J. Cherry, *Solute transport through fractured media : 2. column study of fractured till*, Water Resources Research, 16 (1980), pp. 731–739.

[16] U. Hornung, ed., *Homogenization and Porous Media*, no. 6 in Interdisciplinary Applied Mathematics,, Springer-Verlag, New York, 1997.

[17] U. Hornung and R. Showalter, *Diffusion models for fractured media*, Journal of Mathematical Analysis and Applications, 147 (1990), pp. 69–80.

[18] I. Neretnieks, *Diffusion in the rock matrix : an important factor in radionuclide retardation*, J. Geophys. Res., 85 (1980), pp. 4379–4397.

[19] M. Peszyńska, *Finite element approximation of diffusion equations with convolution terms*, Mathematics of Computation, 65 (1996), pp. 1019–1037.

[20] J. Roberts and J.-M. Thomas, *Mixed and hybrid methods*, in Handbook of Numerical Analysis Vol.II, P. Ciarlet and J. Lions, eds., North Holland, Amsterdam, 1991, pp. 523–639.

[21] T. Russell and M. F. Wheeler, *Finite element and finite difference methods for continuous flows in porous media*, in The Mathematics of Reservoir Simulation, R. E. Ewing, ed., SIAM, Philadelphia, 1984, pp. 35–106.

[22] J. Warren and P. Root, *The behavior of naturally fractured reservoirs*, Soc. Pet. Eng., J. 3 (1963), pp. 245–255.